Phase boundary for the chiral transition in (2 + 1)-flavor QCD at small values of the chemical potential

O. Kaczmarek,[1] F. Karsch,[1,2] E. Laermann,[1] C. Miao,[2] S. Mukherjee,[2] P. Petreczky,[2] C. Schmidt,[3,4] W. Soeldner,[3,4] and W. Unger[1,5]

[1]*Fakultät für Physik, Universität Bielefeld, D-33615 Bielefeld, Germany*
[2]*Physics Department, Brookhaven National Laboratory, Upton, New York 11973, USA*
[3]*Frankfurt Institute for Advanced Studies, J. W. Goethe Universität Frankfurt, D-60438 Frankfurt am Main, Germany*
[4]*GSI Helmholtzzentrum für Schwerionenforschung, Planckstr. 1, D-64291 Darmstadt, Germany*
[5]*Institut für Theoretische Physik, ETH Zürich, CH-8093 Zürich, Switzerland*

(Received 26 November 2010; published 10 January 2011)

We determine the chiral phase transition line in (2 + 1)-flavor QCD for small values of the light quark chemical potential. We show that for small values of the chemical potential the curvature of the phase transition line can be deduced from an analysis of scaling properties of the chiral condensate and its susceptibilities. To do so we extend earlier studies of the magnetic equation of state in (2 + 1)-flavor QCD to finer lattice spacings, $aT = 1/8$. We use these universal scaling properties of the chiral order parameter to extract the curvature of the transition line at two values of the cutoff, $aT = 1/4$ and $1/8$. We find that cutoff effects are small for the curvature parameter and determine the transition line in the chiral limit to leading order in the light quark chemical potential. We obtain $T_c(\mu_q)/T_c(0) = 1 - 0.059(2)(4)(\mu_q/T)^2 + \mathcal{O}(\mu_q^4)$.

DOI: 10.1103/PhysRevD.83.014504 PACS numbers: 11.15.Ha, 12.38.Gc, 12.38.Mh, 25.75.Nq

I. INTRODUCTION

Extending lattice QCD calculations to nonzero baryon-chemical potential or, equivalently, to nonzero net baryon number density is known to be difficult in general. However, important information on the QCD phase diagram can be deduced for small values of the chemical potential by using well-established numerical techniques such as reweighting [1], analytic continuation [2,3], or Taylor expansion [4,5]. We will concentrate here on the latter approach.

Not only do Taylor expansions of thermodynamic observables provide information on QCD thermodynamics at small but nonzero chemical potential, the expansion coefficients themselves also are sensitive indicators for critical behavior in the vicinity of the chiral phase transition at vanishing chemical potential. As the chemical potential couples to the quark number current, which does not break chiral symmetry, it acts to leading order like a temperature variable. Derivatives with respect to chemical potentials lead to susceptibilities which exhibit critical behavior similar to that of thermal susceptibilities [6]. We will show here that a calculation of the leading order Taylor expansion coefficient of the chiral order parameter, which defines a mixed susceptibility, allows us to perform quantitative studies of the phase boundary between low and high temperature phases of QCD close to $\mu = 0$.

At nonzero values of the chemical potential a phase boundary in the temperature and chemical potential parameter space of QCD is well defined only in the heavy quark limit or for vanishing quark masses. In the former case the phase transition line corresponds to the first order deconfinement transition in the pure gauge theory. At infinite values of the quark mass this transition is independent of the chemical potential and defines a straight line in the T-μ plane. For a large range of quark mass values the transition line is not unique. It characterizes a region of (rapid) crossover in thermodynamic quantities and a pseudocritical temperature extracted from these observables may differ somewhat, depending on the observable that is used. In the chiral limit, however, the transition line is again well defined. For sufficiently large strange-quark mass it defines a line of second order phase transitions in the universality class of three dimensional $O(4)$ symmetric spin models [7].

Taylor expansions, analytic continuation, as well as reweighting techniques have been used to locate the crossover line $T_c(\mu)$ in the T-μ plane for small values of the chemical potential [8]. These calculations, which have been performed for different flavors and various values of the quark masses, suggest that the curvature is small, i.e., $T_c(\mu)/T_c(0)$ decreases only by a few percent at $\mu/T \simeq 1$. However, so far most lattice QCD calculations performed to determine the transition line have been performed on coarse lattices,[1] i.e., lattices with only four sites in the temporal direction for which the lattice spacing in units of the temperature thus equals $aT = 1/4$. Better control over the extrapolation to the continuum limit and the quark mass dependence of the transition line clearly is needed.

So far studies of the transition line concentrated on its dependence on a single chemical potential, taken to be

[1]An attempt to determine the transition line closer to the continuum limit has been presented in [9].

either identical for the light up (μ_u) and down (μ_d) quarks or of opposite sign. The former is the light quark chemical potential, $\mu_q = (\mu_u + \mu_d)/2$ and the latter is the isospin chemical potential, $\mu_I = (\mu_u - \mu_d)/2$ for which direct numerical calculations are possible. In order to make contact to the situation met in heavy ion collisions [10,11] one eventually wants to analyze the influence of nonzero charge (μ_Q) and strangeness (μ_S) chemical potentials on the curvature of the transition line, i.e., one should allow for nonvanishing up-, down-, and strange-quark chemical potentials. For small values of the chemical potential this is possible in the framework we will outline here. At present we will, however, restrict our discussion to the case of vanishing strange-quark and isospin (electric charge) chemical potentials.

We concentrate on an analysis of the phase transition line in the chiral limit ($m_u = m_d = 0$, $m_s > 0$) where its dependence on μ_q is expected to be largest. We will present a calculation of the critical line for small values of the light quark masses in the scaling regime of the finite temperature chiral phase transition. This allows us to use scaling relations to extract the curvature of the phase transition line in the chiral limit of QCD. The scaling relations naturally relate the curvature of the critical line as a function of μ_q to the magnitude of a mixed susceptibility.

We will perform our numerical calculations for $(2 + 1)$-flavor QCD keeping the heavier strange-quark mass close to its physical value and decreasing the two degenerate light quark masses towards the massless limit. On coarse lattice with temporal extent $N_\tau = 4$ we will make use of a recently performed scaling analysis [12] of the chiral order parameter performed with an improved staggered fermion action. This study showed that the chiral order parameter is well described by a universal scaling function characteristic for a three dimensional, $O(N)$ universality class. As we are using a staggered fermion discretization scheme for our scaling analysis we expect that the transition in the chiral limit, performed at nonzero lattice spacing, is controlled by the $O(2)$ rather than the $O(4)$ universality class. We thus will analyze our numerical results in terms of $O(2)$ scaling functions. We will comment on the application of $O(4)$ scaling relations later on.

This paper is organized as follows. In the next section we will extend the scaling analysis of the chiral order parameter to lattices with temporal extent $N_\tau = 8$. This provides the basic parameters needed for a calculation of the curvature of the chiral phase transition line which will be discussed in Sec. III. We give a discussion of our results and an outlook in Sec. IV.

II. MAGNETIC EQUATION OF STATE

In the vicinity of a critical point regular contributions to the partition functions become negligible in higher order derivatives and the singular behavior of response functions will generally be dominated by contributions arising from the singular part of the free energy density[2]

$$f(T, m_l, m_s, \mu_q, \mu_s) = f_s(T, m_l, m_s, \mu_q, \mu_s) + f_r(T, m_l, m_s, \mu_q, \mu_s). \quad (1)$$

In addition to the temperature T, light (m_l), and strange (m_s) quark masses we also allow for a dependence of the free energy density on the quark chemical potentials. Close to the chiral phase transition temperature at vanishing chemical potential the singular part f_s will give rise to universal scaling properties of response functions. This has been exploited to analyze basic universal features of the QCD phase diagram close to criticality [13].

The singular part of the free energy density depends on the parameters of the QCD Lagrangian, e.g., the quark masses, and the external control parameters, temperature and chemical potentials, only through two relevant couplings. These scaling variables, t and h, control deviations from criticality, $(t, h) = (0, 0)$, along the two relevant directions, which in the case of QCD characterize fluctuations of the energy and chiral condensate, respectively. To leading order the scaling variable h depends only on parameters that break chiral symmetry in the light quark sector, while t depends on all other couplings. In particular, t will depend on the light quark chemical potential while h remains unaffected by these in leading order,

$$t \equiv \frac{1}{t_0}\left(\frac{T - T_c}{T_c} + \kappa_q\left(\frac{\mu_q}{T}\right)^2\right), \qquad h \equiv \frac{1}{h_0}\frac{m_l}{m_s}, \quad (2)$$

where T_c is the phase transition temperature in the chiral limit and t_0, h_0 are nonuniversal scale parameters (as is T_c). While the combination $z_0 = h_0^{1/\beta\delta}/t_0$ is unique for a given theory, the values of t_0 and h_0 will change under the rescaling of the order parameter [12]. Note also that they depend on the definition of the parameter introduced to control symmetry breaking, i.e., the fact that we choose the strange-quark mass to normalize the symmetry breaking light quark mass parameter. For the rest of this chapter we will not need to refer any further to the contribution of chemical potentials to the reduced temperature t. We will come back to it in the next chapter.

The singular part of the free energy, f_s, is a homogeneous function of its arguments. This can be used to rewrite it in terms of the scaling variable $z = t/h^{1/\beta\delta}$ as

$$f_s(t, h) = h^{1+1/\delta} f_s(z, 1) \equiv h^{1+1/\delta} f_s(z), \quad (3)$$

where β, δ are critical exponents of the three dimensional $O(N)$ universality class [14,15], $\beta = 0.349$ and $\delta = 4.780$ for three dimensional $O(2)$ models and $\beta = 0.380$ and

[2]For systems belonging to the 3-dimensional $O(2)$ or $O(4)$ universality classes this does not hold for the thermal response function (specific heat) as the relevant critical exponent α is negative in these cases.

$\delta = 4.824$ for $O(4)$, respectively. All parameters entering the definition of t and h, i.e., t_0, h_0, and T_c may depend on the strange-quark mass, but are otherwise unique in the continuum limit of $(2 + 1)$-flavor QCD. Just like the transition temperature T_c, however, t_0 and h_0 are also cutoff dependent and will need to be extrapolated to the continuum limit.

The universal critical behavior of the order parameter, $M \sim \partial f/\partial m_l$, is controlled by a scaling function f_G that arises from the singular part of the free energy density after taking a derivative with respect to the light quark mass,

$$M(t, h) = h^{1/\delta} f_G(z). \tag{4}$$

The scaling function $f_G(z)$ is well known for the $O(2)$ and $O(4)$ universality classes through studies of three dimensional spin models [16]. This so-called magnetic equation of state, Eq. (4), has been analyzed recently for $(2 + 1)$-flavor QCD using an improved staggered fermion formulation (p4-action) on lattices with temporal extent $N_\tau = 4$ [12] and light quark masses as small as $m_l/m_s = 1/80$, which corresponds to a pion mass that is about half its physical value. It could be shown that the chiral order parameter can be mapped onto a universal $O(N)$ scaling curve and the scale parameters t_0, h_0, T_c could be extracted. As the calculations had been performed with staggered fermions the scaling analysis has been performed by comparing results with the magnetic equation of state for a $O(2)$ universality class rather than $O(4)$ as one should find in the continuum limit for two massless quark flavors. However, as has been argued in [12] both scaling curves are similar in the limited range of z values, where this scaling analysis has been performed, and the scaling analysis could have been performed with $O(4)$ scaling functions as well.

At least on these coarse $N_\tau = 4$ lattices violations of scaling have been found to be small also for physical values of the light quark mass, i.e., $m_l/m_s \simeq 1/27$. Of course, it is to be expected that the scale parameters, extracted on coarse lattices with temporal extent $N_\tau = 4$, are subject to cutoff effects. We therefore extend the analysis of Ref. [12] to smaller lattice spacings. We perform calculations on lattices with temporal extent $N_\tau = 8$. We follow here the discussion presented in Ref. [12] and introduce two order parameters that are multiplicatively renormalized by multiplying the chiral condensate with the strange-quark mass, but differ in handling additive divergences, linear in the quark mass,[3]

$$\begin{aligned} M_b &\equiv N_\tau^4 \hat{m}_s \langle \bar{\psi}\psi \rangle_l, \\ M &\equiv N_\tau^4 \hat{m}_s \left(\langle \bar{\psi}\psi \rangle_l - \frac{m_l}{m_s} \langle \bar{\psi}\psi \rangle_s \right). \end{aligned} \tag{5}$$

We use in our study data for the chiral condensate which have been collected by the hotQCD [17] and RBC-Bielefeld [18] Collaborations in their studies of the $(2 + 1)$-flavor equation of state on lattices of size $32^3 \times 8$ as well as in the course of analyzing the transition temperature in $(2 + 1)$-flavor QCD [19]. These calculations have been performed with the p4-action [20] for three different quark mass ratios $m_l/m_s = 0.2$, 0.1, and 0.05, respectively. We use subsets of these data samples which cover a small temperature interval close to the transition region, but also cover the region of the transition temperature in the chiral limit. For the smallest quark mass ratio this includes a set of 16 values of the gauge coupling which cover a temperature interval $0.950.3 \lesssim T/T_c \lesssim 1.12$ $(3.48 < 6/g^2 < 3.545)$. Typically (20.000–30.000) trajectories of 0.5 time units have been generated for each set of quark masses and gauge couplings. The temperature scale used in our scaling analysis is based on calculations of the scale parameter r_0 that have been determined from calculations of the heavy quark potential performed on lattices of size 32^4 [17,18].

The basic approach for the scaling analysis on $N_\tau = 8$ lattices is identical to that described in Ref. [12]. However, as the calculations on the $N_\tau = 8$ lattices have not been performed for as small light quark masses as in the $N_\tau = 4$ analysis [12], where the smallest ratio was $m_l/m_s = 1/80$, we did not perform a separate analysis for the determination of scaling parameters in the small mass regime and a determination of scaling violating terms for larger values of the quark masses, as it has been done in Ref. [12]. We perform a simultaneous analysis of data obtained for all three quark mass ratios and include scaling violating regular terms in the ansatz for scaling fits,

$$M(t, h) = h^{1/\delta} f_G(t/h^{1/\beta\delta}) + a_l \Delta T H + b_1 H + b_3 H^3, \tag{6}$$

with $\Delta T = (T - T_c)/T_c$ and $H = m_l/m_s$. This includes all the scaling violating terms also used on $N_\tau = 4$ lattices. In our final analysis, however, we will set $b_3 = 0$.

We verified that this approach, applied to the $N_\tau = 4$ data set, and restricted to the same mass range available now on $N_\tau = 8$ lattices, i.e., $1/20 \leq m_l/m_s \leq 1/5$, leads to results compatible with our earlier findings. We extract values for t_0, h_0, and T_c which are similar to those obtained previously. In fact, results for fit parameters obtained from the analysis of different order parameters, M and M_b, turn out to be in even better agreement. Results of this new scaling analysis for the $N_\tau = 4$ data set is shown in the upper half of Fig. 1. All fit parameter are summarized in Table I.

[3]At finite values of the cut off these terms are, of course, finite and may be viewed as a specific contribution to the regular part that will not alter the scaling properties for sufficiently small values of the quark mass.

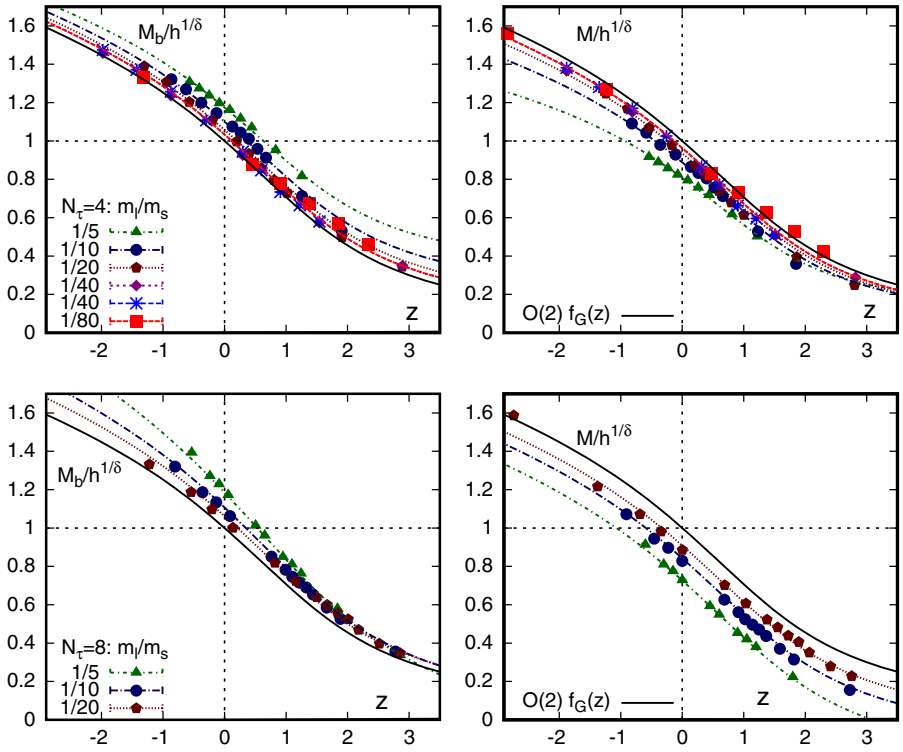

FIG. 1 (color online). Fit of the $O(2)$ scaling function to numerical results for the subtracted order parameter M (right) and the nonsubtracted light quark condensate M_b (left), both for $N_\tau = 4$ (top) and $N_\tau = 8$ (bottom). The fits include an ansatz for violations of scaling as discussed in the text. Shown are results for $m_l/m_s \leq 1/5$.

Using the approach described above for the analysis of our $N_\tau = 8$ data set we find good agreement of fit parameters extracted from an analysis of M_b and M, respectively. Results of this scaling analysis are shown in the lower half of Fig. 1. All fit parameters are summarized in Table I. As already noted in the analysis performed on lattices with temporal extent $N_\tau = 4$ [12], we observe also for $N_\tau = 8$ that scaling violations are small for $m_l/m_s \leq 1/10$. This confirms that physical quark mass values, corresponding to $m_l/m_s \simeq 1/27$, are in the scaling region.

The constants h_0, t_0 determined for $N_\tau = 8$ take on values different from those for $N_\tau = 4$. The invariant combination of scale parameters,

$$z_0 \equiv h_0^{1/\beta\delta}/t_0 = z_0(m_s) + \mathcal{O}(a^2), \tag{7}$$

TABLE I. Scale parameters determined from the scaling fits on lattices of temporal extent $N_\tau = 4$ and 9. In columns 6 and 7 we list the couplings for the leading scaling violating corrections. The last column gives $z_0 \equiv h_0^{1/\beta\delta}/t_0$. We give the results for parameters entering the definition of scaling functions for M_b and the subtracted order parameter M as defined in Eq. (5). Only the former has been used in the analysis of the mixed susceptibilities. Note that fits including regular terms give consistent determinations of the parameters of the scaling functions determined from M_b and M, respectively.

N_τ	M_i	t_0	h_0	$T_c(0)$ [MeV]	a_t	b_1	z_0
			Fit using the scaling term only				
4	M_b	0.0037(2)	0.0022(3)	194.5(4)	⋯	⋯	6.8(5)
	M	0.0048(5)	0.0048(2)	195.6(4)	⋯	⋯	8.5(8)
			Fit using scaling and regular terms				
4	M_b	0.004 07(9)	0.002 95(22)	194.9(2)	3.8(21)	2.1(1)	7.5(3)
	M	0.004 01(9)	0.002 71(20)	194.8(2)	11.2(21)	−2.4(1)	7.2(3)
8	M_b	0.002 71(21)	0.000 48(9)	174.1(8)	−10.1(16)	3.3(5)	3.8(5)
	M	0.003 02(22)	0.000 59(10)	175.1(8)	−0.9(15)	−4.6(4)	3.8(4)

changes by about 50% which shows that its continuum extrapolation is not yet possible. This also is the case for t_0 and h_0 separately.

When comparing results obtained for $N_\tau = 4$ and $N_\tau = 8$ one also has to take into account the dependence of the scale parameters on the strange-quark mass. In fact, as the scaling analysis has been performed at bare strange-quark mass values m_s, fixed in lattice units, the corresponding physical value in the chiral limit at $t = 0$ is only determined *a posteriori*, once T_c has been determined. It turns out that the physical values of the strange-quark mass in the $N_\tau = 4$ and 8 calculations differ at T_c by about 10%. One may account for this mismatch by reweighting the results for the chiral condensates in the light and strange-quark masses [21]. However, we will not attempt to do this here.

The main outcome of the $N_\tau = 8$ scaling analysis, aside from confirming the good scaling properties of the order parameter at a twice smaller value of the lattice spacing, is a determination of the scale parameters and the transition temperature T_c in the chiral limit, needed in the definition of the scaling variable z, i.e., the determination of t_0, h_0, and T_c. We summarize these results in Table I. In the next section we will make use of these scale parameters to determine the curvature of the phase transition line for small values of the quark chemical potential.

III. CURVATURE OF THE CRITICAL LINE

As outlined in the beginning of the previous section at leading order the light quark chemical potential only enters the reduced temperature t, as introduced in Eq. (2). Also at nonvanishing values of the quark chemical potential the phase transition point is located at $t = 0$. The variation of the transition temperature with chemical potential therefore is parametrized in terms of the constant κ_q introduced in Eq. (2),

$$\frac{T_c(\mu_q)}{T_c} = 1 - \kappa_q \left(\frac{\mu_q}{T}\right)^2 + \mathcal{O}\left(\left(\frac{\mu_q}{T}\right)^4\right). \tag{8}$$

To determine the chiral phase transition line in the T-μ plane we thus need to determine the proportionality constant κ_q. This is, in fact, the only left over free parameter in universal scaling functions that needs to be determined. All other parameters $[t_0,\ h_0,\ T_c \equiv T_c(\mu_q = 0)]$ have already been determined in the scaling analysis of the order parameter discussed in the previous section.

The constant κ_q can be determined by analyzing the dependence of the chiral condensate on the light quark chemical potential. Of course, at vanishing light quark mass one would simply determine the temperature at which $\langle\bar{\psi}\psi\rangle_l$ vanishes. At nonzero but small values of the quark mass this information is encoded in scaling functions. To extract information about the dependence of the scaling variable t on κ_q it suffices to consider the leading order Taylor expansion coefficient of the chiral condensate,

$$\frac{\langle\bar{\psi}\psi\rangle_l}{T^3} = \left(\frac{\langle\bar{\psi}\psi\rangle_l}{T^3}\right)_{\mu_q=0} + \frac{\chi_{m,q}}{2T}\left(\frac{\mu_q}{T}\right)^2 + \mathcal{O}((\mu_q/T)^4), \tag{9}$$

where

$$\frac{\chi_{m,q}}{T} = \frac{\partial^2\langle\bar{\psi}\psi\rangle_l/T^3}{\partial(\mu_q/T)^2} = \frac{\partial\chi_q/T^2}{\partial m_l/T}. \tag{10}$$

The mixed susceptibility $\chi_{m,q}$ is proportional to the leading order coefficient of the Taylor expansion of the chiral condensate, which has been introduced in [22,23]. It may also be viewed as the quark mass derivative of the light quark number susceptibility (χ_q). Details of its definition in terms of inverses of the staggered fermion matrix and its derivatives with respect to the quark chemical potential are given in Appendix A of Ref. [23]. We have summarized the formulas relevant for our current analysis in an Appendix.

In the massless limit the chiral order parameter vanishes at T_c and varies as $M \sim (-t)^\beta$. Its derivative with respect to t thus will diverge at T_c like $t^{\beta-1}$. The same singular behavior will thus show up in a derivative of the chiral condensate with respect to temperature as well as the second derivative with respect to μ_q/T. The prefactors of the singularity in $\mathrm{d}M/\mathrm{d}T$ and $\mathrm{d}^2M/\mathrm{d}(\mu_q/T)^2$, however, will differ by a factor $2\kappa_q T_c$. We will make use of this relation to determine the curvature of the critical line at $\mu_q = 0$.

In the vicinity of the critical point the mixed susceptibility can be expressed in terms of the scaling function $f_G'(z) \equiv \mathrm{d}f_G(z)/\mathrm{d}z$,

$$\frac{\chi_{m,q}}{T} = \frac{2\kappa_q T}{t_0 m_s} h^{-(1-\beta)/\beta\delta} f_G'(z). \tag{11}$$

The scaling function $f_G'(z)$ is easily obtained from $f_G(z)$ by using the implicit parametrization for the latter given in Ref. [16]. We also note that $\chi_{m,q}$ diverges as a function of the light quark mass at $t = 0$, i.e., at the chiral phase transition temperature. In contrast to the chiral susceptibility, $\chi_m \sim \partial M/\partial m_l$, which stays finite in the chiral limit only for $t > 0$, the mixed susceptibility is finite for all $t \neq 0$; for $t < 0$ it scales like $(-t)^{\beta-1}$ while for $t > 0$ it behaves like $ht^{-1-\gamma}$.

For small values of the light quark mass numerical results for the mixed susceptibilities $\chi_{m,q}$ may be compared to the right-hand side of Eq. (11). Here all parameters that enter $f_G'(z)$ are known and the only undetermined parameter is κ_q. As we did for the analysis of the magnetic equation of state, we should consider the influence of scaling violations induced by nonzero values of the light quark masses on the determination of the curvature of the phase transition line. The leading

quark mass corrections identified in the analysis of the magnetic equation of state will not contribute to $\chi_{m,q}$ as they do not depend on the chemical potential. The first scaling violating term would arise from a regular term that gives corrections to the order parameter of the form $M \sim a_q H(\mu_q/T)^2$. This would give rise to corrections to the scaling relation given in Eq. (11)

$$t_0 h^{(1-\beta)/\beta\delta} \frac{m_s}{T} \frac{\chi_{m,q}}{T} = 2\kappa_q f_G'(z) + \frac{2a_q h_0^{1/\delta}}{z_0} H^{1+(1-\beta)/\beta\delta}. \tag{12}$$

As we do not know the prefactor a_q we need to check in the analysis of the mixed susceptibilities whether corrections to scaling play a role. We note, however, that in the case of the magnetic equation of state the dominant corrections arise from the term $b_1 H$, which is ultraviolet divergent in the continuum limit. This term drops out in the analysis of $\chi_{m,q}$. Moreover, scaling violating terms are further suppressed by a factor $H^{(1-\beta)/\beta\delta} \equiv H^{0.39}$ [or $H^{0.34}$ in $O(4)$ symmetric models] as the dominant scaling term itself is divergent at $(t, h) = (0, 0)$. We thus expect scaling violations to be small.

Using a subset of the data samples described in the previous section, we calculated the mixed susceptibility $\chi_{m,q}$ on lattices with temporal extent $N_\tau = 4$ for several values of the quark mass. For this analysis we used data sets separated by 50 trajectories. For the lightest quark mass ratio, $m_l/m_s = 1/80$, we selected 4 and for the 3 heavier quark mass ratios, $m_l/m_s = 1/10, 1/20, 1/40$, we choose 6 values of the gauge coupling in a narrow temperature interval close to the chiral phase transition temperature T_c, i.e., $-0.02 \leq (T - T_c)/T_c \leq 0.06$. Typically this involved about 500 to 950 gauge field configurations per parameter set, except for the lightest quark mass ratio where we analyzed about 350 gauge field configurations. On each gauge field configuration we calculated the various operators necessary to construct $\chi_{m,q}$. An explicit expression for them is given in the Appendix (see also Appendix A of [23]).

The calculation of the various operators required inversions of the staggered fermion matrix with a large set of random noise vectors. We used 500 noise vectors on each gauge field configuration and constructed unbiased estimators for the various traces that need to be calculated. All these calculations could be performed very efficiently on a graphics processing unit (GPU) cluster.

Results obtained for the mixed light quark number susceptibility, $\chi_{m,q}$, on lattices with temporal extent $N_\tau = 4$ are shown in Fig. 2. We clearly see that $\chi_{m,q}$ increases in the transition region with decreasing values of m_l/m_s.

Using the scaling relation given in Eq. (11) we can rescale the data and obtain a unique scaling curve. This scaling curve can be mapped onto the $O(2)$ scaling function $f_G'(z)$ with a simple multiplicative rescaling factor, $2\kappa_q$. The resulting scaling plot is shown in Fig. 3. To check for possible contributions from scaling violating terms we have analyzed the data separately for quark mass ratios $m_l/m_s = 1/10$, $1/20$ and $m_l/m_s = 1/40$, $1/80$. These fits agree within statistical errors. We then determine the curvatures κ_q from fits to the complete data set. Results of these fits are summarized in Table II.

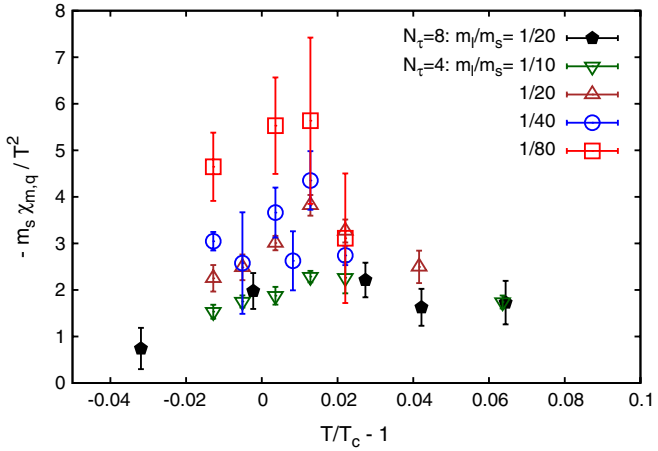

FIG. 2 (color online). The mixed light quark number susceptibility as a function of the reduced temperature, $(T - T_c)/T_c$. Shown are results obtained at two values of the cutoff, $N_\tau = 4$ (open symbols) and $N_\tau = 8$ (filled symbols), and for several values of the light to strange-quark mass ratio.

The scaling analysis performed for the mixed susceptibility on lattices with temporal extent $N_\tau = 4$ suggests that the determination of the curvature parameter κ_μ can be reliably performed with quark masses $m_l/m_s \lesssim 1/10$. This is in accordance with the scaling analysis of the order parameter itself, which we have discussed in the previous

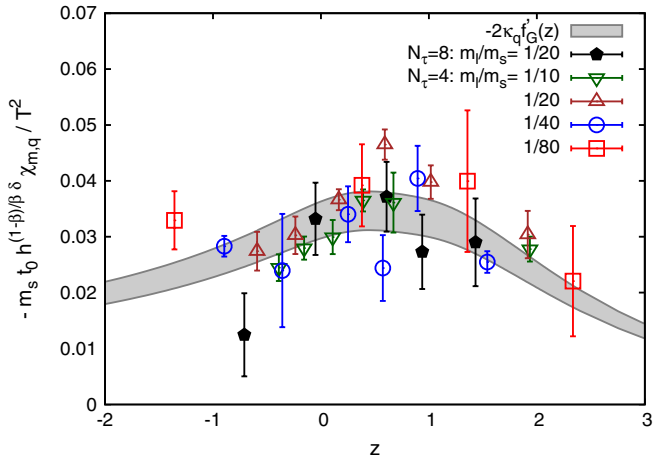

FIG. 3 (color online). The scaled mixed susceptibility as function of the scaling variable $z = t/h^{1/\beta\delta}$. The data are compared to the $O(2)$ scaling curve. The band shows a 10% error band on this curve which arises from statistical errors on the calculated observables as well as from the errors on the scaling parameters t_0 and z_0 given in Table I.

TABLE II. Determination of the curvature of the critical surface of the chiral phase transition in (2 + 1)-flavor QCD as function of the light quark chemical potential μ_q. The table summarizes fits performed separately for two lighter and two heavier quark mass sets as well as the combined data set.

N_τ	m_l/m_s	κ_q	χ^2/dof
4	1/10, 1/20	0.0598(26)	3.5
	1/40, 1/80	0.0573(29)	1.5
8	1/20	0.0559(35)	0.4
4, 8	all	0.0591(17)	2.1

section. It thus seems to be safe to extract the curvature parameter also at smaller values of the lattice spacing, i.e., from our $N_\tau = 8$ data set, by using the smallest quark mass ratio available there, $m_l/m_s = 1/20$. We have performed calculations at five values of the temperature using gauge field configurations on $32^3 \times 8$ lattices generated by the hotQCD Collaboration [19]. For these parameter sets we have analyzed 300 to 600 gauge field configurations, which were separated by 100 trajectories. Again we used 500 noise vectors for the calculation of all relevant operators on each of the gauge field configurations. The result of this analysis is shown in Figs. 2 and 3 with filled symbols. As can be seen they agree well with results obtained on coarser lattices.

When rescaling data obtained for $\chi_{m,q}$ to the $O(2)$ scaling curve $f'_G(z)$ we need to take into account errors on the scaling parameters t_0 and z_0 (or h_0). This leads to a 10% error for the determination of the curvature terms.

Performing a combined fit to all results obtained for different quark mass values and lattice spacings we obtain

$$\kappa_q = 0.059(2)(4). \tag{13}$$

This result for the curvature of the critical line is about a factor of 2 larger than the reweighting results obtained in (2 + 1)-flavor QCD [1]. It is however consistent with results obtained in calculations with imaginary chemical potentials. In fact it lies in between the 2-flavor [2] and 3-flavor [24] simulations performed with the standard staggered fermion formulation and also is consistent with results reported from (2 + 1)-flavor simulations with imaginary chemical potential performed with the action used also in this study (p4-action) [25].

IV. CONCLUSIONS

With this analysis we have established a systematic way to determine the curvature of the QCD phase transition line in the chiral limit for small values of the light quark chemical potential. We have determined the curvature for two values of the cutoff using an improved staggered fermion action (p4-action). Within our present statistical accuracy we did not observe any significant quark mass dependence of the scaled mixed susceptibilities. The result observed for the curvature of the second order phase transition line in the chiral limit thus also is a good estimate for the crossover line at physical values of the light quark masses.

Although the final result for the curvature term seems to show little cutoff dependence, one has to be cautious as the other three scale parameters that enter this analysis (t_0, h_0, and T_c) all vary significantly as the lattice spacing is reduced by a factor of 2. Clearly more work is needed to extrapolate safely to the continuum limit. We will do so in the future by repeating the analysis with a discretization scheme that also suppresses cutoff effects arising from taste symmetry violation in the staggered fermion action more efficiently (hisq action).

In our current analysis we have kept the strange-quark and isospin chemical potentials equal to zero. A direct comparison to the situation met in heavy ion collisions on the freeze-out curve thus should be done with caution. However, at least for large energies, i.e., small values of the baryon-chemical potential experimental results for the freeze-out curve correspond to electric charge chemical potentials, which are more than an order of magnitude smaller than μ_B. As susceptibilities obtained by derivatives with respect to strange-quark chemical potentials rather than light quark chemical potentials are generally smaller, one may also expect that the curvature in the μ_S direction will turn out to be smaller. It thus seems that the curvature of the critical surface along the $\mu_q \simeq \mu_B/3$ direction is most relevant for a comparison of lattice QCD results with the experimentally determined freeze-out curve. The phenomenological parametrization of the freeze-out curve given in [11] yields $T_{\rm freeze}(\mu_B)/T_{\rm freeze}(0) \simeq 1 - 0.21(2)(\mu_q/T)^2 + \mathcal{O}(\mu_q^4)$. The curvature of the freeze-out curve thus is about a factor of 4 larger than that determined here for the chiral phase transition curve. This suggests that the freeze-out curve may not follow the chiral phase transition or crossover line at nonzero values of the chemical potential. With increasing μ_q/T the hadronic freeze-out seems to happen further away from criticality. At the largest value of the light quark chemical potential currently explored in the low energy scan at the Relativisitc Heavy Ion Collider [26], $\mu_q/T \simeq 1$, the freeze-out temperature may be about 15% below the crossover temperature.

Nonetheless, as pointed out above, one still needs to improve the current lattice calculations. Results closer to the continuum limit with further improved fermion discretization schemes are needed and one should also get control over the influence of nonvanishing strange-quark chemical potentials in order to firmly establish the separation of the freeze-out curve from the chiral transition line as advocated above.

ACKNOWLEDGMENTS

This work has been supported in part by Contract No. DE-AC02-98CH10886 with the U.S. Department of

Energy, the BMBF under Grant No. 06BI401, the Gesellschaft für Schwerionenforschung under Grant No. BILAER, the Extreme Matter Institute under Grant No. HA216/EMMI and the Deutsche Forschungsgemeinschaft under Grant No. GRK 881. C. S. has been partially supported through the Helmholtz International Center for FAIR which is part of the Hessian LOEWE initiative. Numerical simulations have been performed on the BlueGene/L at the New York Center for Computational Sciences (NYCCS) which is supported by the U.S. Department of Energy and by the State of New York, the GPU cluster of USQCD at Jefferson Laboratory, the GPU cluster SCOUT at the Center for Scientific Computing (CSC) at Frankfurt University, as well as the John von Neumann Supercomputer center (NIC) at FZ-Jülich, Germany. We thank M. Bach for his help in developing the CUDA based programs used for our data analysis on GPU clusters.

APPENDIX: THE MIXED SUSCEPTIBILITY $\chi_{m,q}$

We summarize here the operators entering a calculation of the mixed susceptibility $\chi_{m,q}$ introduced in Eq. (10). This susceptibility is proportional to the second order Taylor expansion coefficient of the chiral condensate in terms of the light quark chemical potentials. Using Appendix A of Ref. [23] we introduce the expectation value of the light quark chiral condensate as

$$\frac{\langle\bar{\psi}\psi\rangle_l}{T^3} = \langle\mathcal{C}_0\rangle, \tag{A1}$$

and obtain for the mixed susceptibility,

$$\begin{aligned}\frac{\chi_{m,q}}{T} &\equiv \frac{\partial^2\langle\bar{\psi}\psi\rangle_l/T^3}{\partial(\mu_q/T)^2}\bigg|_{\mu_q=0} = \frac{1}{N_\tau^2}\frac{\partial^2\langle\bar{\psi}\psi\rangle_l/T^3}{\partial\hat{\mu}^2}\bigg|_{\hat{\mu}=0} \\ &= \frac{1}{N_\sigma^3}(\langle\mathcal{C}_2\rangle + 2\langle\mathcal{C}_1\mathcal{D}_1\rangle + \langle\mathcal{C}_0\mathcal{D}_2\rangle + \langle\mathcal{C}_0\mathcal{D}_1^2\rangle \\ &\quad - \langle\mathcal{C}_0\rangle(\langle\mathcal{D}_2\rangle + \langle\mathcal{D}_1^2\rangle)),\end{aligned} \tag{A2}$$

where we have introduced the shorthand notation $\hat{\mu} = \mu_q a$ for the chemical potential expressed in units of the lattice spacing. Here $\mathcal{C}_n$ and $\mathcal{D}_n$ denote n-th derivatives of the trace of the inverse fermion matrix (D) and logarithms of its determinant, respectively,

$$\mathcal{C}_n = \frac{1}{4}\frac{\partial^n \mathrm{tr} D^{-1}}{\partial\hat{\mu}^n}, \qquad \mathcal{D}_n = \frac{1}{2}\frac{\partial^n \ln\det D}{\partial\hat{\mu}^n}, \tag{A3}$$

where the derivatives are defined with respect to the flavor chemical potential $\hat{\mu} \equiv \hat{\mu}_f$ for the quark flavor f. The factors $1/4$ and $1/2$ arise because we define the mixed susceptibility as a derivative of the 1-flavor light quark chiral condensate with respect to the light quark chemical potential μ_q which is identical for the two light flavor components of the fermion action, i.e., a flavor factor $n_f = 2$ arises only in derivatives of the logarithm of the fermion matrix.

The operators needed to calculate $\chi_{m,q}$ thus are

$$\mathcal{C}_0 = \tfrac{1}{4}\mathrm{tr}(D^{-1}), \tag{A4}$$

$$\mathcal{C}_1 = -\frac{1}{4}\,\mathrm{tr}\left(D^{-1}\frac{\partial D}{\partial\hat{\mu}}D^{-1}\right), \tag{A5}$$

$$\begin{aligned}\mathcal{C}_2 = -\frac{1}{4}\Bigg(&\mathrm{tr}\left(D^{-1}\frac{\partial^2 D}{\partial\hat{\mu}^2}D^{-1}\right) \\ &- 2\,\mathrm{tr}\left(D^{-1}\frac{\partial D}{\partial\hat{\mu}}D^{-1}\frac{\partial D}{\partial\hat{\mu}}D^{-1}\right)\Bigg),\end{aligned} \tag{A6}$$

$$\mathcal{D}_1 = \frac{1}{2}\,\mathrm{tr}\left(D^{-1}\frac{\partial D}{\partial\hat{\mu}}\right), \tag{A7}$$

$$\mathcal{D}_2 = \frac{1}{2}\left(\mathrm{tr}\left(D^{-1}\frac{\partial^2 D}{\partial\hat{\mu}^2}\right) - \mathrm{tr}\left(D^{-1}\frac{\partial D}{\partial\hat{\mu}}D^{-1}\frac{\partial D}{\partial\hat{\mu}}\right)\right). \tag{A8}$$

[1] Z. Fodor and S. D. Katz, J. High Energy Phys. 03 (2002) 014; 04 (2004) 050.
[2] P. de Forcrand and O. Philipsen, Nucl. Phys. **B642**, 290 (2002).
[3] M. D'Elia and M. Lombardo, Phys. Rev. D **67**, 014505 (2003).
[4] C. R. Allton, S. Ejiri, S. J. Hands, O. Kaczmarek, F. Karsch, E. Laermann, and C. Schmidt, Phys. Rev. D **68**, 014507 (2003).
[5] R. V. Gavai and S. Gupta, Phys. Rev. D **68**, 034506 (2003).
[6] S. Ejiri, F. Karsch, and K. Redlich, Phys. Lett. B **633**, 275 (2006).
[7] R. Pisarski and F. Wilczek, Phys. Rev. D **29**, 338 (1984).
[8] For a summary of earlier results on the curvature of the transition line see O. Philipsen, Prog. Theor. Phys. Suppl. **174**, 206 (2008).
[9] G. Endrodi, Z. Fodor, S. D. Katz, and K. K. Szabo, Proc. Sci., LATTICE2008 (2008) 205.
[10] A. Andronic, P. Braun-Munzinger, and J. Stachel, Nucl. Phys. **A772**, 167 (2006).
[11] J. Cleymans, H. Oeschler, K. Redlich, and S. Wheaton, Phys. Rev. C **73**, 034905 (2006).
[12] S. Ejiri *et al.*, Phys. Rev. D **80**, 094505 (2009).
[13] Y. Hatta and T. Ikeda, Phys. Rev. D **67**, 014028 (2003).
[14] J. Engels, S. Holtmann, T. Mendes, and T. Schulze, Phys. Lett. B **514**, 299 (2001).

[15] J. Engels, L. Fromme, and M. Seniuch, Nucl. Phys. **B675**, 533 (2003).
[16] J. Engels, S. Holtmann, T. Mendes, and T. Schulze, Phys. Lett. B **514**, 299 (2001).
[17] A. Bazavov *et al.*, Phys. Rev. D **80**, 014504 (2009).
[18] M. Cheng *et al.*, Phys. Rev. D **81**, 054504 (2010).
[19] A. Bazavov *et al.* (Hot QCD Collaboration) (to be published).
[20] F. Karsch, E. Laermann, and A. Peikert, Phys. Lett. B **478**, 447 (2000).
[21] W. Unger, Ph.D. thesis, Bielefeld, 2010.
[22] S. Gupta and R. Ray, Phys. Rev. D **70**, 114015 (2004).
[23] C. R. Allton *et al.*, Phys. Rev. D **71**, 054508 (2005).
[24] P. de Forcrand and O. Philipsen, J. High Energy Phys. 01 (2007) 077.
[25] R. Falcone, Proc. Sci., LATTICE2010 (2010) 183.
[26] M. M. Aggarwal *et al.* (STAR Collaboration), arXiv:1008.3133.